International Journal of Pharmaceutics 404 (2011) 148–158

Contents lists available at ScienceDirect

International Journal of Pharmaceutics

journal homepage: www.elsevier.com/locate/ijpharm

Spray freeze drying with polyvinylpyrrolidone and sodium caprate for improved dissolution and oral bioavailability of oleanolic acid, a BCS Class IV compound

Henry H.Y. Tong[a], Zhen Du[b], Geng Nan Wang[c], H.M. Chan[a], Qi Chang[c], Leon C.M. Lai[b], Albert H.L. Chow[d,*], Y. Zheng[b,**]

[a] School of Health Sciences, Macao Polytechnic Institute, Macao
[b] Institute of Chinese Medical Sciences, University of Macau, Macao
[c] Institute of Medicinal Plant Development, Chinese Academy of Medical Science & Peking Union Medical College, Beijing 100193, China
[d] School of Pharmacy, The Chinese University of Hong Kong, Hong Kong, China

ARTICLE INFO

Article history:
Received 23 September 2010
Received in revised form
11 November 2010
Accepted 12 November 2010
Available online 19 November 2010

Keywords:
Spray freeze drying
Sodium caprate
Dissolution
Oral bioavailability
Oleanolic acid
Sodium oleanolate

ABSTRACT

Spray-freeze-drying (SFD) of oleanolic acid (OA), a BCS Class IV compound, with polyvinylpyrrolidone-40 (PVP-40) as stabilizer and sodium caprate (SC) as wetting agent and penetration enhancer produced kinetically stable, amorphous solid dispersion systems with superior *in vitro* dissolution performance, and better and more uniform absorption in comparison with commercial OA tablet. Relative to the SC-free formulation, the presence of SC in the formulation resulted in a significant increase in the *in vivo* absorption rate of OA while exerting no apparent impact on the extent of OA absorption. The SFD-processed OA formulations and commercial OA tablet generally exhibited large inter-animal variability in oral bioavailability, consistent with the absorption characteristics of BCS Class IV compounds. Inclusion of SC coupled with the replacement of OA with its sodium salt (OA-Na) in the formulation was shown to substantially decrease the observed absorption variability. Above results suggested that increases in both dissolution rate and intestinal permeability of BCS Class IV compounds, as exemplified by the SFD-processed dispersion system containing both OA-Na and SC, are critical to reducing the large inter-individual absorption variability commonly observed with this class of drugs.

1. Introduction

Oleanolic acid (OA) is a pentacyclic triterpenoid naturally occurring in many Asian herbs, such as *Fructus ligustri lucidi*, *Fructus forsythiae*, *Radix ginseng* and *Akebia trifoliate*. In China, OA is available over the counter in tablet form and has been used for several decades as an adjunct therapy for hepatitis and for the prevention of hepatotoxicity induced by anti-tuberculosis medications such as isoniazid and pyrazinamide (Chen et al., 2005; Tong et al., 2008). According to the Biopharmaceutics Classification System (Amidon et al., 1995; US FDA, 2000), OA should fall in the Class IV category because of its low aqueous solubility (<1 μg/ml) (Tong et al., 2008) and low permeability (P_{app} = 1.1–1.3 × 10^{-6} cm/s in the apical-to-basolateral direction at 10 and 20 μM) (Jeong et al., 2007). In rats, OA has an absolute oral bioavailability of only 0.7% (Jeong et al., 2007). In order to improve the aqueous dissolution rate and/or oral bioavailability of OA, various formulation strategies have been attempted with success in some cases. For instance, preparation of different crystal forms of OA by recrystallization from solutions failed to provide any improvement in dissolution performance (Tong et al., 2008), whereas inclusion complexation with cyclodextrin and solid dispersion in hydrophilic polymers afforded impressive dissolution enhancement (Yan et al., 1995; Neu & Zhao, 2003). However, neither of the latter two systems has been evaluated for oral bioavailability. In addition, nanosuspension formulation of OA showed improvement over OA raw powdered material not only in *in vitro* dissolution rate but also in *in vivo* hepatoprotective effect against carbon tetrachloride induced liver injury (Chen et al., 2005). Employing a self-nanoemulsified drug delivery system composed of OA:Sefsol 218:Cremophor EL:Labrasol (0.2:50:25:25, w/v/v/v), it has been demonstrated that the relative oral bioavailability and mean retention time of OA were about 2.4 times higher than those of commercial OA tablets (Xi et al., 2009). These results have clearly demonstrated that molecular dispersion in an amorphous excipient matrix and particle size reduction are both effective for improving the dissolution and bioavailability of OA. However, in terms of bioavailability enhancement, these formulation approaches still have limitations, since they do not address the problem of poor intestinal permeability with BCS Class IV compounds. In order to fill this void for OA

* Corresponding author. Tel.: +852 26096829; fax: +852 26035295.
** Corresponding author. Tel.: +853 83974687; fax: +853 28841358.
E-mail addresses: albert-chow@cuhk.edu.hk (A.H.L. Chow), yzheng@umac.mo (Y. Zheng).

0378-5173/$ – see front matter © 2010 Elsevier B.V. All rights reserved.
doi:10.1016/j.ijpharm.2010.11.027

formulation, the present study has employed a combination of approaches for improving the oral absorption of OA, encompassing solid dispersion of OA in PVP matrix using spray freeze drying (SFD), conversion of OA to the sodium salt form, and addition of the penetration enhancer, sodium caprate (SC). The former two approaches ensure instantaneous dissolution of OA in water while the last strategy is intended to boost the transport of OA across the intestinal epithelial cells.

The choice of PVP in the present study is guided by its established utility in the formulation of kinetically stable amorphous solid dispersion systems with superior dissolution performance for poorly soluble drugs (Serajuddin et al., 1999). SC is also deemed a judicious excipient choice here for various reasons. Firstly, SC, being a medium chain fatty acid with an excellent safety profile, has already been approved as a safe food additive (US FDA, 2009). Secondly, SC, consisting of a hydrophilic 'head' (carboxylate ion) and a hydrophobic 'tail' (C_{10} chain), is surface active with a critical micelle concentration of 50 mM in pure water at 22–25 °C (Namani & Walde, 2005). This property serves to facilitate wetting and enhance solubilization of the hydrophobic OA in water. Thirdly, SC has been shown to increase the intestinal permeability of a number of poorly absorbable drugs, such as cefotaxime and cyclosporine A (Sharma et al., 2005). Depending on the concentration, SC can act on both transcellular and paracellular transports. The demonstrated effectiveness of SC in cell cultures at low concentrations (<13 mM) may be explained by its specific ability to open the tight junctions between the cells via displacement of the tight junction proteins, such as claudins 4, 5 and occludin, from the lipid rafts in the epithelial membrane (Sugibayashi et al., 2009). On the other hand, the *in vivo* absorption-promoting effect of SC observed at higher concentrations is possibly mediated through its surface activity which augments transcellular transport by destabilizing and solubilizing enterocyte membranes (Maher et al., 2009). Both of these transport-promoting mechanisms are crucial to the formulation of BCS Class IV drugs with acceptable bioavailability.

Apart from solid dispersion of OA in amorphous hydrophilic PVP matrix together with SC, conversion of OA to a water-soluble salt is expected to bring about further dissolution improvement due to an increased ease of ionization in water and the stronger ion–dipole interactions between the ionic form of OA and water. A suitable choice of the salt would be one with a monovalent cation such as Na^+ or K^+, which is readily ionized in water (Chow et al., 2008). Accordingly, the sodium salt of OA (sodium oleanolate) has been selected for bioavailability assessment in the present study.

SFD is a technique of growing popularity for formulating solid pharmaceuticals. A basic SFD process consists of two major steps, viz. spray-freezing on cryogenic liquid surface (Maa and Nguyen, 2001), or into cryogenic liquid (Williams III et al., 2005), followed by freeze-drying in a conventional freeze-drier. Since the whole SFD process is conducted under sub-ambient conditions, it is particularly suited for drying heat-labile materials. SFD has been successfully employed to enhance the *in vitro* dissolution rate and *in vivo* oral bioavailability of poorly soluble compounds, such as carbamazepine (Hu et al., 2002, 2003) and danazol (Rogers et al., 2002a,b, 2003a,b; Hu et al., 2004a; Vaughn et al., 2006). SFD-processed pharmaceutical powders are generally amorphous, porous, micron-sized, and occasionally with nano-structures, which accounts for their exceptionally high dissolution rate (Hu et al., 2002, 2003, 2004a,b; Rogers et al., 2003a,b).

The primary goal of the present study is to develop a consistent, stable and efficacious oral OA solid dispersion dosage form using SFD technology. As modern combinatorial chemistry in pharmaceutical research tends to yield mostly BCS Class IV molecules and most reported formulation studies employing SFD processing focused on BCS Class II compounds (with low solubility and high permeability), the present study aimed to assess the utility of SFD processing in conjunction with the aforementioned formulation strategies in improving the oral bioavailability of BCS Class IV compounds.

2. Materials and methods

2.1. Materials

Standard OA (minimum purity 97%) was purchased from Sigma (St. Louis, USA), and standard glycyrrhetinic acid (≥98%) was obtained from National Institute for the Control of Pharmaceutical and Biological Products (Beijing, China). Pharmaceutical grade OA raw material (OA-RW) (purity ≥ 95%) was purchased from International Laboratory (San Bruno, USA). Polyvinylpyrrolidone-40 (PVP-40) of pharmacopoeial grade, sodium caprate (purity ≥ 98%) and sodium hydroxide were purchased from Sigma (St. Louis, USA). Sodium dodecyl sulphate was purchased from USB Corporation (Cleveland, USA). All organic solvents (butan-1-ol, acetonitrile, methanol, ethanol, dichloromethane, chloroform, acetonitrile, ethyl ether and acetone) used were of either analytical or HPLC grade, and purchased from Merck, Germany. Water used was purified by a Milli Q-water purification system of Millipore Corporation (Bedford, USA).

2.2. Preparation of OA samples by spray-freeze-drying (SFD)

The compositions of all formulations prepared by spray-freeze-drying are tabulated in Table 1. Spray-freeze-dried OA samples were prepared by spraying the feed solutions at defined compositions (Table 1) via a twin-fluid nozzle in a Mini Spray Dryer B290 (Buchi, Switzerland) above the surface of liquid nitrogen in an insulating tank (Fig. 1). A minimum distance of 4 cm was kept between the nozzle and liquid nitrogen surface to prevent nozzle clog. The solution feed rate was set at 20 ml min^{-1}, and the atomization pressure of nitrogen gas was kept at 4 bar. Stirring of the feed solution was maintained by a magnetic bar during the spray freezing process. Once the spray-freezing step was completed, the content was carefully transferred to a freeze dryer (CoolSafe™, ScanLaf A/S Company, Denmark), and maintained at room temperature under a vacuum pressure of 45.3 Pa for 24 h. The average product yield per SFD run was 86.9 ± 3.1%. Physical mixtures (PM) of OA and PVP serving as the "control" samples for the various SFD-processed OA formulations at 1:1 weight ratios were prepared by simple physical mixing inside a sealed plastic bag for 10 min.

Sodium oleanolate (OA-Na) used in one of the SFD-processed formulations was synthesized as follows: 6 g OA was refluxed in 200 ml 95% (v/v) ethanol with 1.04 g NaOH at 100 °C for 30 min. The solution was then cooled to room temperature, and concentrated to approximately 30 ml by rotary evaporation (Rotary Evaporator R-210, Buchi, Switzerland) at 60 °C and −120 mbar. The resulting OA-Na precipitate was then filtered, repeatedly washed with cold deionized water, tray-dried at 80 °C for 1 day, and stored at 25 °C over silica gel for 1 month prior to analysis.

All freeze-dried OA powders produced were similarly stored over silica gel until further characterization.

2.3. Scanning electron microscopy (SEM)

After gold coating in Scancoat Six SEM sputter coater (Edwards, UK) under vacuum, OA samples were characterized for surface morphology using a scanning electron microscope (Model: JSM 6300F, JEOL, Japan) at 1000–75,000× magnification.

Table 1
Formulation composition by physical mixing, spray-drying and spray-freeze-drying in this study.

Formulations	OA (g)	OA-Na (g)	PVP40 (g)	SC (g)	n-butanol (ml)	Ethanol (ml)	Water (ml)
SFD OA Formula A	0.2	–	–	–	60	40	100
SFD OA:PVP (1:1) Formula B	0.2	–	0.2	–	60	40	100
SFD OA:PVP (1:9) Formula C	0.2	–	1.8	–	60	40	100
SFD OA-Na:PVP (1:1) Formula D	–	0.2	0.2	–	60	40	100
SFD PVP:SC (1:2) Formula E	–	–	0.2	0.4	60	40	100
SFD OA:PVP:SC (1:1:2) Formula F	0.2	–	0.2	0.4	60	40	100
SFD OA-Na:PVP:SC (1:1:2) Formula G	–	0.2	0.2	0.4	60	40	100

2.4. X-ray photoelectron spectroscopy

Elemental surface compositions of selected OA samples were assessed by a Perkin-Elmer Physical Electronics 5600 spectrometer (Massachusetts, USA), using a monochromatic Al Kα X-ray source for energy resolution analysis under vacuum conditions. All spectra were recorded over a range of binding energy from 0 to 1400 eV, with a pass energy of 187.85 eV for the wide scan survey spectra and pass energy of 58.70 eV for high energy spectra for the regions of C1s, N1s, O1s, Na1s and K2p. After the energy calibration of C1s peak position at 285.0 eV was completed, the elemental compositions of each material were determined using the corresponding relative sensitivity factors and Multipak peak fitting software.

2.5. Powder X-ray diffraction (PXRD) and variable-temperature powder X-ray diffraction (VT-PXRD)

Selected OA samples were gently packed into sample holders. PXRD patterns were recorded with a Philips powder X-ray diffraction system, Model PW 1830, using a 3 kW Cu anode (λ = 1.540562 Å) over a 2θ interval of 2.0° to 40.0°. The step size was 0.05°, with a counting time of 2 s.

VT-PXRD patterns were recorded using a Panalytical, X'pert Pro diffractometer with an ultra-fast X-ray detector (X'celerator, USA). The measurements were carried out with CuKα radiation (λ = 1.540562 Å) at 40 kV and 40 mA. The scanning was conducted in the continuous mode over a 2θ range from 5.0 to 40.0° in increments of 0.0338°. Once the minimum vacuum was established inside the sample chamber, VT-PXRD patterns were recorded at every 10 °C increment from 30 to 180 °C.

2.6. Thermal analysis

Differential scanning calorimetry (DSC) was performed using a DSC TA Q1000 system (New Castle, USA). Indium (T_m = 156.6 °C; ΔH_f = 28.45 J g^{-1}) was used for calibration. Accurately weighed samples (~1.5–2.0 mg) were placed in sealed pin-holed aluminum pans and scanned at 10 °C min^{-1} from 50 to 350 °C under nitrogen purge.

Thermal gravimetric analysis (TGA) was performed in an open pan using a TGA TA Q5000 system (New Castle, USA). Approximately 10 mg of the material (accurately weighed) was scanned at 10 °C min^{-1} from 50 to 350 °C.

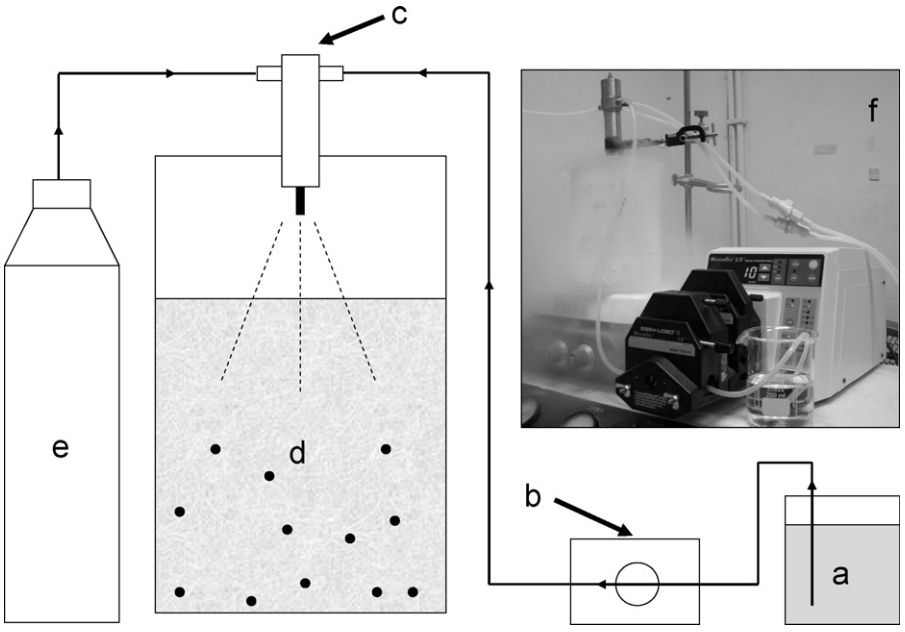

Fig. 1. Schematic diagram of SFD experimental setup. (a) Feed solution; (b) peristaltic pump; (c) two-fluid nozzle; (d) liquid nitrogen container; (e) high pressure gas source; (f) SFD setup.

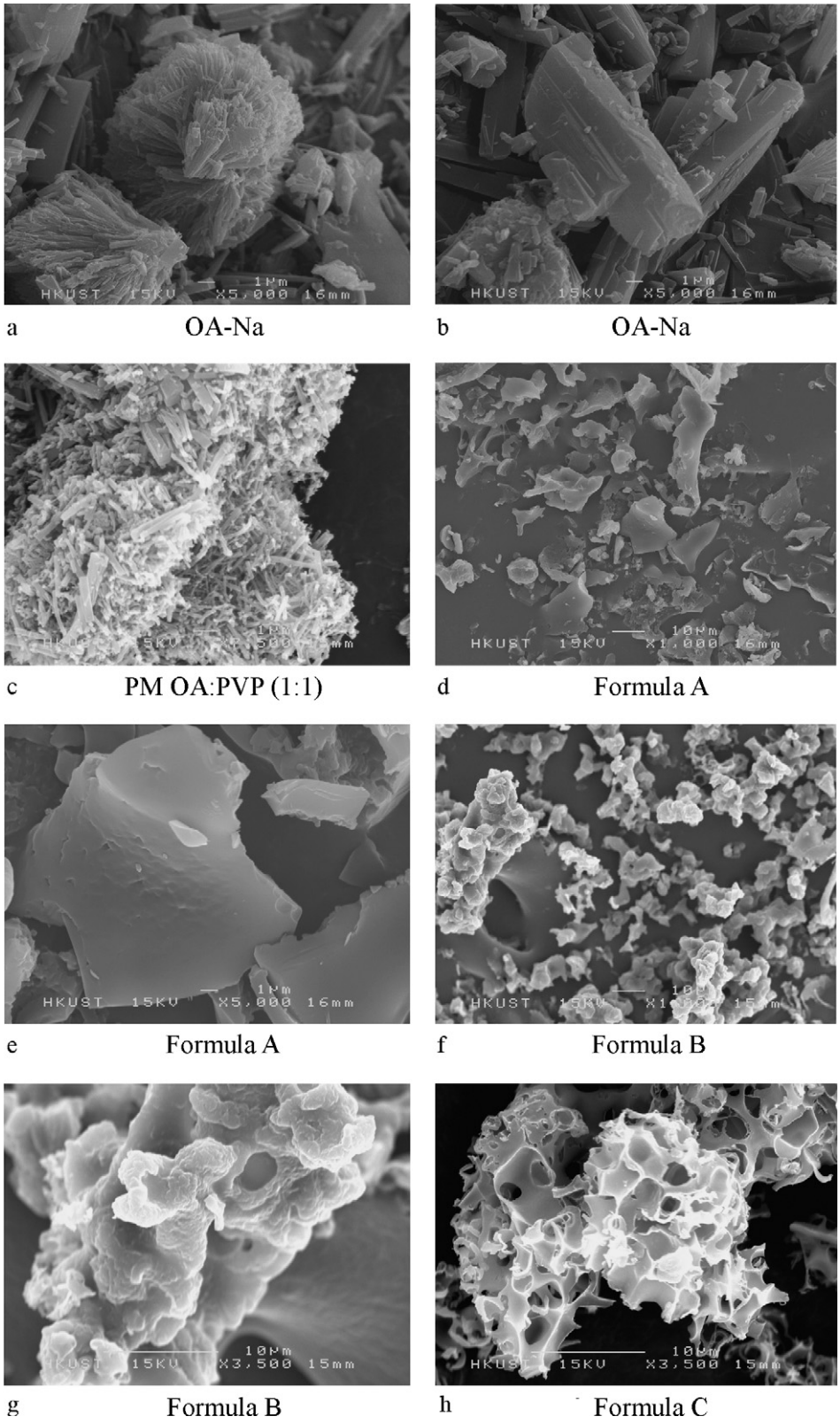

Fig. 2. SEM of PM and SFD OA formulations. (a) and (b): OA-Na; (c): PM OA:PVP (1:1); (d) and (e): Formula A; (f) and (g): Formula B; (h): Formula C; (i) and (j): Formula F; (k) and (l): Formula G.

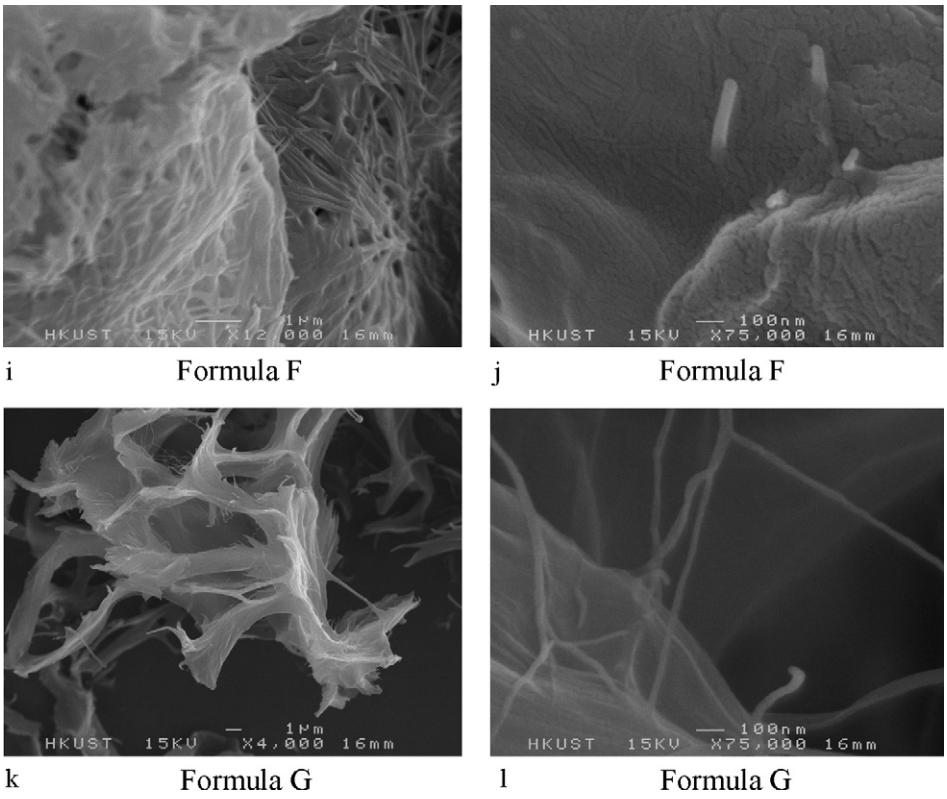

i Formula F j Formula F

k Formula G l Formula G

Fig. 2. *(Continued.)*

2.7. Surface area analysis

Specific surface area was determined by BET nitrogen adsorption using an Autosorb-1 Series surface area analyzer (Quantachrome, USA). Samples were placed in glass sample holders and outgassed with helium at 40 °C for 6 h before analysis. Nitrogen was used as the adsorbate, and 11 BET points were recorded for specific surface area determination.

2.8. HPLC analysis

HPLC analysis of OA was conducted as reported previously (Tong et al., 2008; Xi et al., 2009). An Agilent 1100 series HPLC system (Santa Clara, USA) equipped with 250 mm × 4.6 mm Agilent 5 μm Zorbax® SB-C18 column and photodiode array detector was employed. Mobile phase, composed of acetonitrile and 0.5% phosphoric acid in water (85:15, v/v), was eluted isocratically at 1.0 ml min^{-1}. Twenty-microlitre samples were injected. A calibration curve based on the area ratio of the OA (2–64 μg/ml) and glycyrrhetinic acid (internal standard; 32 μg/ml) peaks detected at 204.0 nm exhibited excellent linearity ($R^2 > 0.999$). The detection limit for OA in this assay was 1 μg/ml. The RSDs of intra- and inter-day precision and accuracy for OA at three different concentrations (4, 32, and 64 μg/ml) were less than 5% ($n = 5$).

2.9. GC–MS analysis

GC–MS analysis of residual butan-1-ol in samples was performed using an Agilent 6890 gas chromatograph coupled to an Agilent 5973 mass spectrometer and an Agilent ChemStation (Agilent Technologies, Palo Alto, CA). A capillary column (30 m × 0.25 mm i.d.) coated with 0.25 μm film of 5% phenyl methyl siloxane was used for separation. The injection volume was 2 μl. The split ratio was 500:1. The oven and injector temperatures were maintained at 40 °C and 200 °C, respectively. Helium was used as the carrier gas at a flow rate of 1 μl min^{-1}. The mass spectrometer was operated with the following settings: electron-impact (EI) mode, scan range at 40–550 amu, ionization energy at 70 eV, and scan rate at 0.34 s per scan. The quadrupole and ionization source were maintained at 150 and 280 °C, respectively.

2.10. Powder dissolution study

Powder dissolution study was performed using a standard USP dissolution tester (DT 706 1000LH, Erweka, Germany). Sample, containing an equivalent amount of 20 mg or 40 mg OA, was added to 900 ml water with or without 1% (w/v) sodium dodecyl sulphate (SDS). The temperature was controlled at 37.0 ± 0.5 °C, and paddle speed was maintained at 100 rpm. At appropriate time intervals (5, 10, 20, 30, 45, 60 and 120 min), samples (5 ml) were withdrawn, filtered through a 0.22 μm membrane filter, and assayed for OA concentration by HPLC as specified in the preceding section. An equal volume of fresh dissolution medium was added to maintain the volume constant after each sample withdrawal. All dissolution runs were performed in triplicate.

2.11. Stressed stability assessment

Representative SFD-processed OA powders were stored inside glass vials with silica gel desiccant at 40 °C for stability assessment. Samples were removed at the end of 1, 2, 3, 6 months for PXRD, HPLC analysis and powder dissolution testing.

2.12. In vitro transport studies using Caco-2 cell monolayer

The *in vitro* intestinal permeability of OA, with or without sodium caprate, was investigated using a Caco-2 cell monolayer model. To avoid the precipitation of calcium caprate, Ca^{2+}-free

phosphate buffer solution (PBS) was used as the medium in the transport studies with sodium caprate as described previously (Zhou et al., 2009). To ensure the integrity of the Caco-2 cell monolayer, transepithelial electrical resistance (TEER) was measured using EVOM & EVOMX Epithelial Voltohmmeters (World Precision Instruments, Inc., USA) before and after each permeability experiment. In the control group, 1.5 ml of 4 μg/ml OA in Ca^{2+}-containing phosphate buffer solution (PBS^{+}) was loaded at the apical side, and 2.6 ml of blank PBS^{+} was loaded at the basolateral side. In the treatment group, 1.5 ml of 4 μg/ml OA in PBS (Ca^{2+}-free buffer) with 0.06% (w/v) sodium caprate, and 2.6 ml of blank PBS were loaded at the apical and basolateral sides respectively. After 2 h, the solutions obtained from the basolateral side in the receiver chamber were freeze-dried, and re-constituted with methanol and water (50:50, v/v). The resulting solutions were sonicated for 20 min (to ensure complete dissolution), centrifuged at 13,000 rpm for 5 min, and analyzed by HPLC as described before.

2.13. In vivo bioavailability assessment in Sprague–Dawley rats

The bioavailability study protocol of Xi et al. (2009) was followed with slight modifications. The animal experiment was approved by the Animal Ethics Committee of the Institute of Medicinal Plant Development, Chinese Academy of Medical Sciences (Beijing, China). Male Sprague–Dawley rats (210 ± 10 g), supplied by Vital River Experimental Animal Co. Ltd. (Beijing, China), were housed under standard laboratory conditions, and granted free access to standard rodent diet and water before the experiment. After cannulation of its jugular vein by polyethylene catheters for blood sampling, the rat was housed individually, allowed to recover for 24 h and then fasted overnight prior to drug dosing. SFD-processed OA formulations were given orally to SD rats ($n = 5$) at OA equivalent 50.0 mg/kg by gastric gavages. The blood samples (0.2 ml) were withdrawn via the catheter before and at 5, 15, 30, 60, 90, 120, 180, 240, 360, 480, and 720 min post-dosing, and immediately placed into heparinized tubes. After centrifugation at 4000 rpm for 5 min, the plasma (100 μl) was collected and stored at −20 °C until assay. After each blood sample collection, the catheter was immediately flushed with 0.2 ml injection of normal saline containing 20 IU of heparin to prevent blood coagulation.

Plasma concentration of OA was determined by liquid chromatography/mass spectrometry/mass spectrometry (LC/MS/MS) as previously described (Xi et al., 2009). Plasma concentrations versus time profiles were analyzed using WinNonlin software (Pharsight Corporation, Mountain View, CA, USA, Version 2.1). For individual rat in each group, non-compartmental model was employed to estimate the following pharmacokinetic parameters: peak plasma concentration (C_{max}), the time to reach C_{max} (T_{max}), area under the plasma concentration versus time curve from zero to last sampling time point ($t = 12$ h) ($AUC_{0\to t}$), and mean retention time (MRT). The pharmacokinetic parameters of the SFD-processed formulations were then compared with those of the commercial OA tablet reported previously (Xi et al., 2009).

3. Results and discussion

3.1. Physical characteristics of sodium oleanolate

Sodium oleanolate (OA-Na) employed in one of the SFD-processed formulations was first prepared and characterized as described in Section 2.

Particle morphology of the prepared OA-Na is presented in Fig. 2a and b. The particles were rod-shaped crystals with a large specific surface area (Table 2) and a PXRD pattern that is distinctly different from those of OA-RW (Fig. 3a) and the non-solvate and solvate forms of OA reported previously (Tong et al., 2008). The material also displayed a prominent endotherm at 50–150 °C and a broad and shallow endotherm at 162.4–236.3 °C in DSC. The first endotherm probably corresponded to dehydration of the sodium salt (Fig. 4), since the associated mass loss (7.58%) within the same temperature range in TGA accorded well with the theoretical water content for a dihydrate salt form (7.00%). Furthermore, the

Table 2
Surface areas of selected OA samples.

Samples	Surface area (m^2/g)	n
OA-RW	3.52	1
OA-Na	48.39 ± 0.39	3
Formula B	4.23	1
Formula C	1.39	1
Formula F	9.50 ± 0.19	3
Formula G	18.06 ± 0.12	3

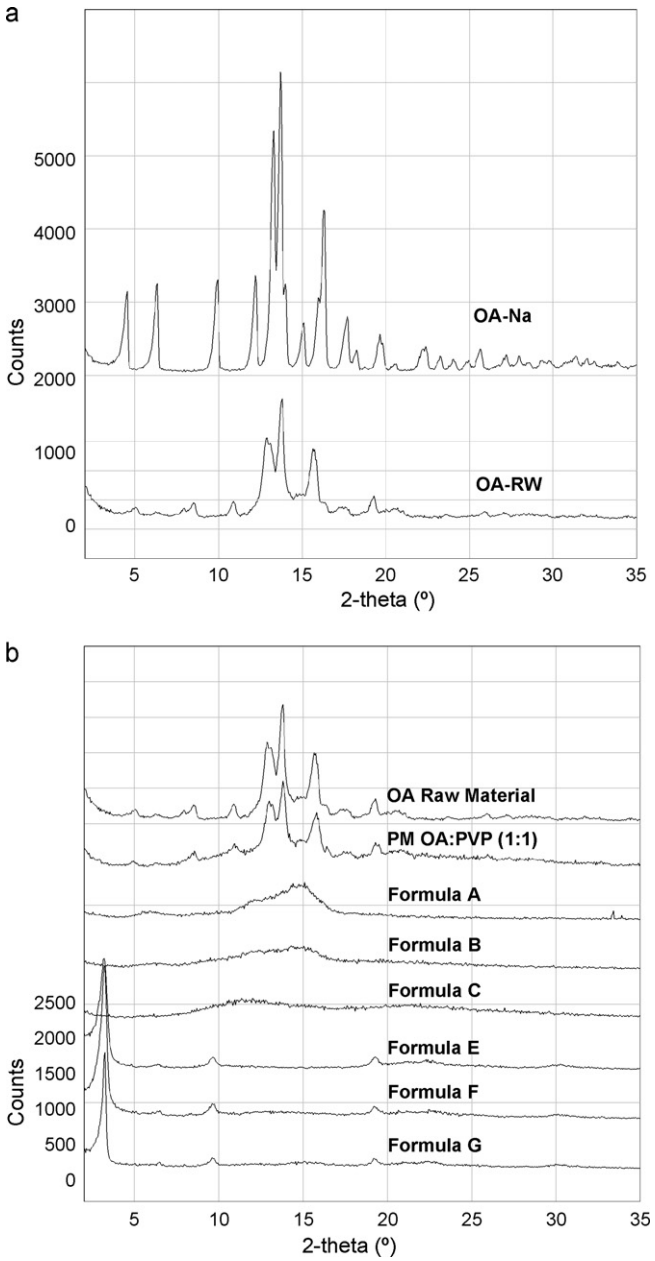

Fig. 3. (a) PXRD patterns of OA-RW and OA-Na. (b) PXRD patterns of PM- and SFD-processed OA formulations.

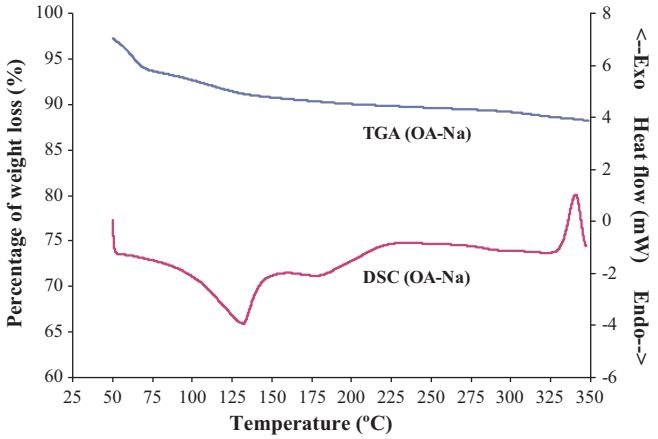

Fig. 4. DSC and TGA curves of OA-Na.

observed OA content of the dihydrate salt (86.18 ± 1.60%; $n = 3$), as analyzed by HPLC, was also close to the theoretical value (88.73%). The dehydration of OA-Na at around 40–50 °C was further substantiated by VT-PXRD conducted under a mild vacuum by stepwise temperature increment from room temperature to 180 °C (Fig. 5). The second endotherm in DSC was possibly due to the melting of the anhydrous salt which remained partially amorphous immediately following dehydration. This deduction was based on the facts that the transition was not accompanied by any weight loss at the same temperature range in TGA (Fig. 4) and that a partial loss in crystallinity of the anhydrate was also observed in VT-PXRD at 130–180 °C (Fig. 5). In addition, upon storage of the OA-Na material at 25 °C over saturated sodium chloride solution (75%RH) or pure water (100%RH) for 1 month, the PXRD pattern characteristic of crystalline OA-Na dihydrate remained essentially unchanged at all RHs studied (data not shown).

3.2. In vitro permeability enhancement with sodium caprate

OA permeability was assessed in the absence and presence of SC using a Caco-2 monolayer cell model, and the data are summarized in Table 3. The presence of 0.06% (w/v) SC (~3.1 mM) augmented the permeation of OA through the Caco-2 cell monolayer in 2 h by 2.76 times ($p < 0.05$) with a concomitant reduction in TEER, indicative of an increased transport through the paracellular route via opening of the cellular tight junctions. As the OA concentration accumulating on the basolateral side during the first hour of the transport study was too low for reliable quantification, only the sample collected at 2 h was assayed for OA content. Assuming a linear transport of OA across the monolayer during the whole 2-h incubation period, the permeability coefficients of OA estimated for both the control and SC treatment groups were roughly in the order of 1×10^{-7} cm/s, comparable to that of the paracellular marker, lucifer yellow ($1.63 \pm 0.12 \times 10^{-7}$ cm/s, Zhang et al., 2004). This implies that the observed permeability increase of OA with ~3.1 mM SC is limited only to the paracellular pathway. While the causes for the poor membrane permeability of OA have yet to be elucidated, there is some evidence to suggest that the efflux system may be involved in limiting the transcellular transport of OA. As shown by Najar et al. (2010), OA exhibited a concentration-dependent stimulatory effect on P-glycoprotein ATPase activity, indicative indirectly of OA being a substrate of P-glycoprotein.

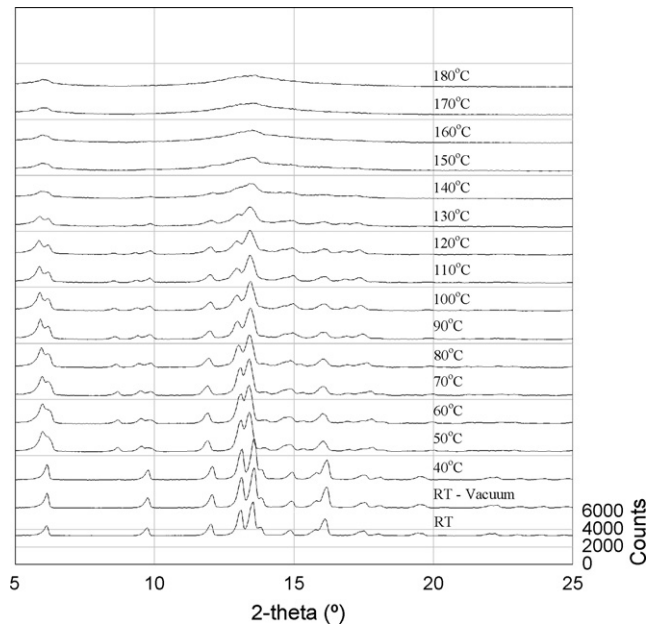

Fig. 5. VT-PXRD patterns of OA-Na.

Table 3
Effects of sodium caprate on OA transport through Caco-2 cells.

Group	OA transported in 2 h (μg)	OA transported in 2 h (%)
Control	0.138 ± 0.023	3.68 ± 0.61
0.06% (w/v) SC	0.381 ± 0.053*	10.16 ± 1.40*

* $p < 0.05$ in 1-tailed Student's t-test, compared with control.

Table 4
Summary of XPS results in selected OA samples.

	C (%)	N (%)	O (%)	Na (%)
Formula B	83.92 (82.97)	6.04 (6.23)	10.04 (10.79)	0.00 (0.00)
Formula C	78.23 (76.60)	10.56 (11.24)	11.21 (12.16)	0.00 (0.00)
Formula E	76.86 (76.25)	1.88 (4.37)	12.82 (14.38)	8.44 (5.00)
Formula F	78.01 (80.06)	0.73 (3.23)	12.46 (13.00)	8.80 (3.70)
Formula G	78.60 (79.93)	1.07 (3.27)	12.21 (13.05)	8.12 (3.75)

Remark: Number in bracket indicates the theoretical atomic ratios for totally homogenous part.

3.3. Particle morphology, physical properties and stability of spray-freeze dried samples

Particle morphology of the 1:1 physical mixture of OA-RW and PVP, i.e., PM OA:PVP (1:1), serving as a control sample is presented in Fig. 2c. In terms of particle size, PVP particles were larger than the OA-RW ones, and OA-RW particles tended to aggregate on the surface of PVP particles. The morphologies of the various SFD-processed OA materials were distinctly different from one another. Spray-freeze dried OA without any PVP (i.e., Formula A; Table 1) appeared as large clumps (Fig. 2d and e) while sample containing 1:1 (w/w) of OA and PVP (i.e., Formula B; Table 1) was fused particulates (Fig. 2f and g), and sample with 1:9 (w/w) of OA and PVP (i.e., Formula C; Table 1) was sponge-like (Fig. 2h). Samples comparison between Formula B and Formula F (Table 1) showed

Table 5
Residual amounts of butan-1-ol of selected OA samples.

Samples	Residual amount of butan-1-ol (ppm)
OA-RW	31.74
OA-Na	0.00
Formula B	10.30
Formula C	10.57
Formula F	0.48
Formula G	1.95

that inclusion of SC led to substantial changes in particle morphology (Fig. 2f and g, i and j). Nano-structures in the form of minute interlocking acicular crystals (Fig. 2j and l) were present on the surfaces of all SFD-processed OA formulations with SC, but were absent in both SC-free Formula B and Formula C samples (Fig. 2f–h). These nano-structures are a result of the SC being recrystallized during or after the SFD-process, as evidenced by emergence of the characteristic peaks of crystalline SC in the PXRD patterns of all SC-containing SFD-processed samples, including Formula E (Table 1; Fig. 3b). SC was evidently not incorporated into the amorphous PVP matrix during SFD processing. Replacement of OA with OA-Na in the formulation (i.e., Formula F versus Formula G; Table 1) resulted in more irregular morphology with increased surface corrugation (Fig. 2k and l), consistent with the observed increase in specific surface area (Table 2).

PXRD analysis of the PM-OA:PVP(1:1) sample yielded diffraction peaks characteristic of crystalline OA-RW only, reflecting two separate phases for OA-RW and PVP (Fig. 3b). In contrast, all spray-freeze dried samples of OA with or without PVP (i.e., Formulas A–C) displayed diffuse halo diffraction patterns (Fig. 3b), reflecting a single, homogeneous, essentially amorphous phase. On the other hand, the PXRD patterns of the SC-containing samples (i.e., Formulas E–G) showed only the characteristic diffraction peaks of crystalline SC, indicating that OA or OA-Na remained amorphous in the particles while SC recrystallized at the particle surface.

To determine the distribution of PVP in the various SFD-processed OA samples, XPS, which measures the elemental composition of superficial surface layer with a depth between 2 and 10 nm, was employed. Since nitrogen atom is present only in PVP but not in OA, the atomic ratio of this element can be used to estimate the amount of PVP present on the surface of the samples. XPS data showed that the SFD-processed OA/PVP particles were reasonably homogeneous, as their surface compositions were generally in agreement with the theoretical estimates for a totally amorphous, homogeneous OA/PVP solid dispersion system (Table 4). However, for the SC-treated samples where the SC was found to recrystallize out on the SFD-processed particle surface, XPS data revealed a significantly higher Na content than the theoretical estimate for homogeneous distribution (Table 4). The data also indicated that PVP was less concentrated on the particle surface of these samples, as the associated atomic ratio of N was considerably lower than the corresponding estimate for homogeneous incorporation (Table 4).

The tendency for SC to accumulate and recrystallize at the particle surface can be explained by its surfactant property. Being surface active, SC was located mainly on the surface of the droplets upon atomization during the initial spraying phase, and underwent recrystallization in the subsequent freeze-drying phase. The results accord with the widely reported finding that surfactants (e.g., Tween 80) are adsorbed preferentially at the air-liquid interface of the atomized droplets (Millqvist-Fureby et al., 1999). Upon contact with liquid nitrogen, the atomized droplets were instantaneously frozen by the ultra-fast heat transfer rate, thereby arresting further molecular re-arrangement in the frozen particles. SC remained at frozen droplet surface, and recrystallized out during the primary and secondary drying phases of the freeze-drying process.

It is also worth noting that compared with the OA raw material (OA-RW), the residual butan-1-ol contents in all SFD-processed OA materials (particularly the SC-treated samples) are substantially lower (Table 5). This is probably attributable to the prolonged and efficient drying provided by SFD under the action of the operating vacuum. The levels of residual butan-1-ol in these samples are well below the permissible limit for Class 3 solvents (5000 ppm; Option 1) (Badens et al., 2009), and are regarded as pharmaceutically acceptable. This further highlights the documented advantage of SFD in the removal of residual organic solvents from the processed materials (Badens et al., 2009).

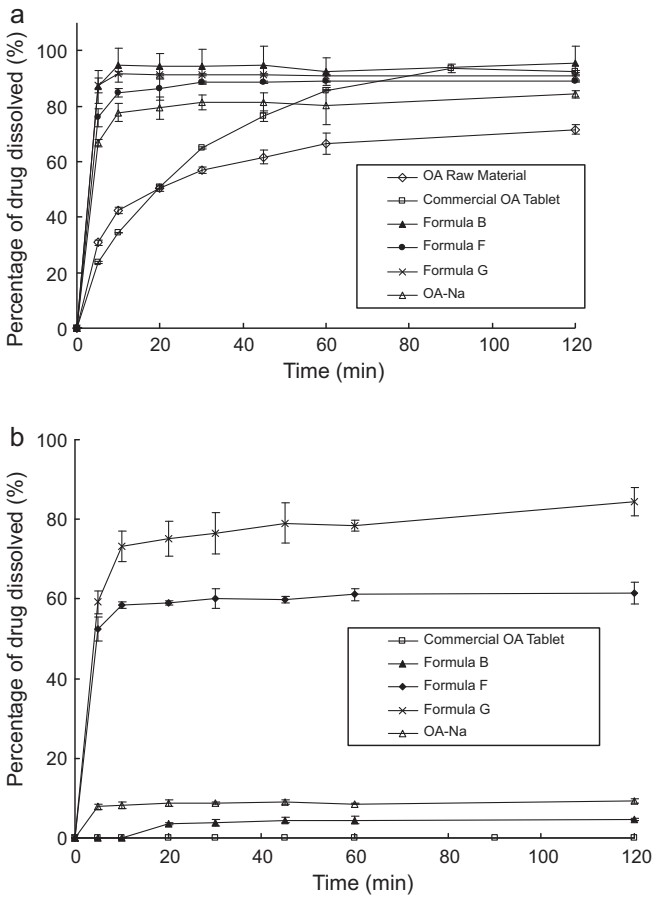

Fig. 6. (a) Powder dissolution profiles of OA raw materials, commercial OA tablet, OA-Na and SFD-processed OA formulations in 1% SDS solution. (b) Powder dissolution profiles of commercial OA tablet, OA-Na, and SFD-processed OA formulations in pure water.

Since amorphous solid dispersion system is thermodynamically unstable and tends to revert to its stable crystalline state, stressed stability testing was conducted on three representative samples, viz. Formulas B, C and F at 40 °C over silica gel. Results showed good kinetic stability of these samples over a period of 6 months, as attested by their insignificant changes in OA content, percent of OA dissolved in 1% SDS solution or water at 10 min and 2 h (Table 6a–c), and PXRD pattern (data not shown).

3.4. Dissolution performance

The dissolution–time profiles of the various samples are presented in Fig. 6. As anticipated from its amorphous nature and high thermodynamic activity, Formula B sample demonstrated a substantially more rapid dissolution than the starting OA raw material (OA-RW) in 1% SDS dissolution medium (Fig. 6a), despite the comparable specific surface areas of these two powdered materials (Table 2). Formula B had more than 80% OA dissolved within 5 min, compared with ~30% for OA-RW, and ~25% with commercial OA tablets (Fig. 6a). However, if pure water was employed as the dissolution medium instead, the SFD-processed sample had less than 5% of OA dissolved at 120 min (Fig. 6b). The results indicated that inadequate wetting was probably responsible for the poor dissolution performance of the sample in surfactant-free water, which could be rectified by adding a wetting agent such as SDS to the dissolution medium. This finding also lends support for the inclusion in the present OA formulation of a surface active agent such as SC, which is normally required to aid the dissolution of hydrophobic drugs by

Table 6
Summary of stability test in SFD-processed OA formulations.

Time (months)	% of OA dissolved within 10 min	% of OA dissolved within 2 h	OA content (%)
(a) Formula B[a]			
0	94.8 ± 6.0	95.3 ± 6.1	42.18 ± 2.54
1	92.3 ± 3.0	91.5 ± 4.6	43.84 ± 1.77
2	94.4 ± 3.4	93.8 ± 5.1	44.10 ± 1.47
3	90.2 ± 0.8	91.2 ± 0.2	44.68 ± 1.78
6	91.1 ± 5.6	87.8 ± 5.8	44.07 ± 2.60
Time (months)	% of OA dissolved within 10 min	% of OA dissolved within 2 h	OA content (%)
(b) Formula C[a]			
0	91.7 ± 4.7	97.8 ± 1.7	9.34 ± 0.21
1	86.0 ± 0.4	85.5 ± 3.2	9.43 ± 1.10
2	84.1 ± 1.9	86.7 ± 2.9	9.68 ± 0.48
3	85.3 ± 1.5	89.3 ± 2.9	9.49 ± 0.74
6	90.0 ± 6.4	89.2 ± 6.2	9.18 ± 1.52
Time (months)	% of OA dissolved within 10 min	% of OA dissolved within 2 h	OA content (%)
(c) Formula F[b]			
0	58.4 ± 0.9	61.5 ± 2.7	21.35 ± 0.18
1	59.0 ± 0.9	61.8 ± 1.3	22.85 ± 1.07
2	60.8 ± 4.7	63.4 ± 2.7	21.64 ± 1.32
3	57.9 ± 0.9	59.5 ± 1.3	23.21 ± 1.40
6	55.5 ± 8.6	59.6 ± 7.4	21.69 ± 0.69

[a] Dissolution medium is 1% SDS solution.
[b] Dissolution medium is pure water.

promoting their initial wetting. As expected, inclusion of SC in the SFD-processed OA formulations brought about an increase of OA dissolved in water from 3.5% (for Formula B) to 59.1% (for Formula F) within 20 min (Fig. 6b).

Despite its substantially higher equilibrium solubility than the free acid, OA-Na itself only showed minimal dissolution improvement in pure water with 7.8 ± 0.7% and 9.3 ± 0.5% dissolved at 5 min and 120 min respectively, compared with 0% dissolution over the same time period for OA-RW. However, in 1% SDS aqueous medium, OA-Na exhibited a much higher rate and extent of dissolution than OA-RW (Fig. 6a). This again stresses the importance of including a surface-active agent in the formulation for overcoming the resistance to initial wetting. Since OA-Na indeed has a much better dissolution performance than the OA free acid in the presence of a surfactant, the co-formulation of OA-Na with SC, both a surfactant and a penetration enhancer, was considered worthwhile for further assessment. As shown in Fig. 4b, the dispersion system formulated with both OA-Na and SC (i.e., Formula G) afforded superior *in vitro* aqueous dissolution performance among all SFD-processed OA formulations (Fig. 6a and b).

3.5. Bioavailability enhancement

Presented in Fig. 7 are the plasma concentration–time profiles of the SFD-processed formulations assessed in the present study and of the commercial OA tablets reported previously (Xi et al., 2009). The related pharmacokinetic parameters are summarized in Table 7.

As shown in Fig. 7a, the plasma concentration–time curve of Formula B was similar in shape to that of the commercial tablets, but the mean plasma concentrations at various time points of the former were all higher than those of the latter. However, because of the large standard deviations of replicate measurements with different animals, the computed mean plasma concentrations and related pharmacokinetic parameters (T_{max}, C_{max}, $AUC_{0\rightarrow t}$, MRT) revealed no statistically significant differences between the two formulations (Table 7). Such large absorption variability is typical of lipophilic but poorly membrane-permeable drugs, i.e., BCS Class IV drugs, which are generally not well absorbed over the intestinal mucosa and tend to show larger inter- and intra-subject variability (Karalis et al., 2008).

Comparison of the plasma concentration–time profiles of Formulas B and G revealed that addition of SC resulted in an initial boost of OA concentration in the plasma, reaching a peak within the first 13–18 min and dropping progressively thereafter, indicative of a rapid dissipation of the impact of SC on OA absorption. In addition, the presence of SC reduced T_{max} by 73% and MRT by 52%, and increased C_{max} by 149% while having no apparent effect on the $AUC_{0\rightarrow t}$ (Table 7). Above data suggest that the absorption-enhancing effect of SC is transitory and reversible, which is perhaps

Table 7
Summary of pharmacokinetic data in three SFD-processed OA formulations.

	Commercial OA tablet (Xi et al., 2009)	Formula B	Formula F	Formula G
T_{max} (min)	48 ± 27	48 ± 27	13 ± 10*	16 ± 9*
C_{max} (ng ml^{-1})	104.93 ± 61.79	160.50 ± 112.25	399.36 ± 188.71*	348.91 ± 166.93*
$AUC_{0\rightarrow t}$ (ng min ml^{-1})	14,974.89 ± 10,906.19	40,216.98 ± 31,860.38[b]	31,067.44 ± 17,840.92[c]	32,657.41 ± 11,832.92*
MRT (min)	138 ± 43	192 ± 37	92 ± 37*	121 ± 28
Rel. BA[a] (%)	100.00	268.56	207.46	218.08
RSD (%)	72.83	79.22	57.43	36.23

* $p < 0.05$ in 1-tailed Student's t-test, compared with commercial OA tablet.
[a] Relative bioavailability, compared with commercial OA tablet.
[b] p value is 0.066.
[c] p value is 0.062.

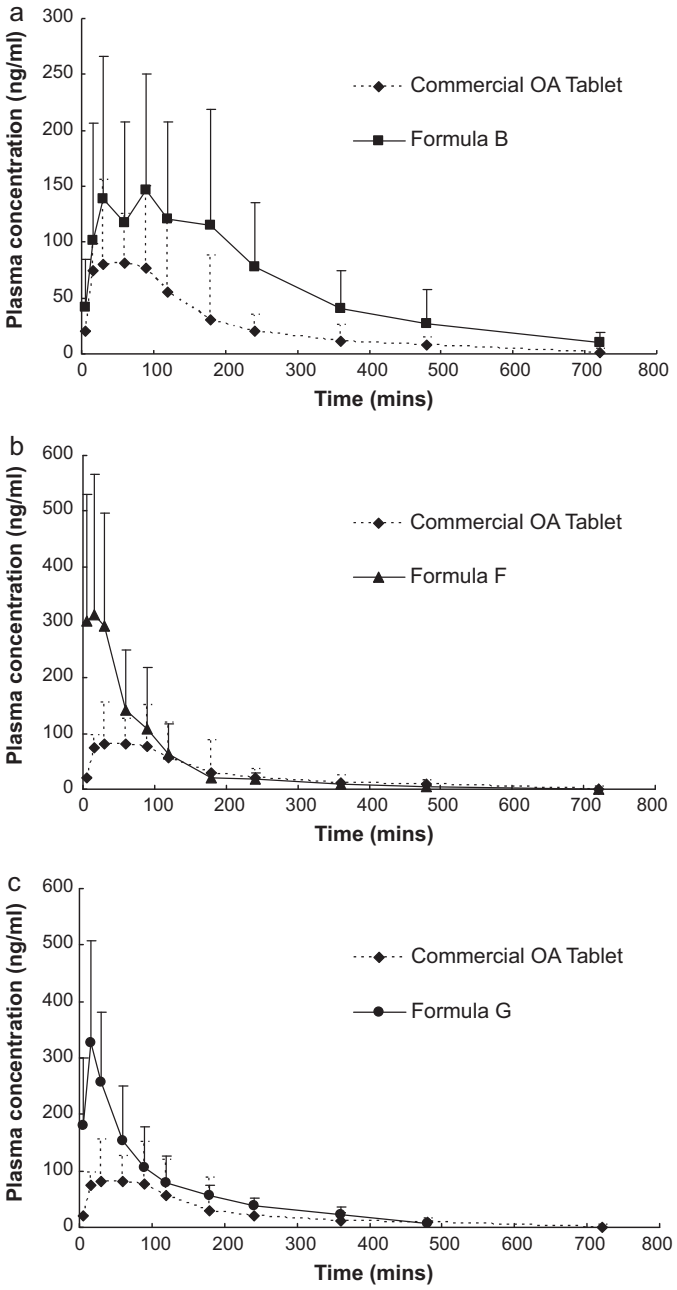

Fig. 7. Plasma concentration–time curves of the three SFD-processed OA formulations.

not unexpected, considering the fact that SC is rapidly dissolvable and readily absorbable in the gastrointestinal tract with an observed T_{max} of less than 10 min in pigs (Raoof et al., 2002). Upon arrival in the gastrointestinal tract, SC, being present on the surface of the samples, would undergo dissolution first prior to the release of OA. The dissolved SC would then act on the intestinal epithelial membrane to promote the absorption of OA, but since SC itself could also be rapidly absorbed from the gastrointestinal tract as aforementioned (Raoof et al., 2002), its impact on the concurrent absorption of OA would decline swiftly in tandem with its own absorption, thus accounting for the insignificant changes in the overall extent of OA absorption.

The influence of the sodium salt form on the oral bioavailability of OA was assessed by comparing the plasma concentration–time profiles and associated kinetic data of Formulas F and G. As shown in Fig. 7b, c and Table 7, replacement of OA with its sodium salt (OA-Na) did not exert any statistically significant impact on either the plasma concentration–time profile or the associated kinetic parameter estimates. This suggests that the use of the OA sodium salt here, though capable of providing a much more rapid dissolution rate in water, offers no additional advantage in terms of bioavailability enhancement. However, it is worth noting that the co-formulation of OA-Na with SC could markedly reduce the variability in both plasma concentrations and oral bioavailability of OA (Fig. 7c, Table 7). For both the commercial tablet and Formula B that were devoid of any penetration enhancer, the RSD of relative bioavailability was high, being 73% and 79% respectively. However, with SC in the formulation, the RSD of relative bioavailability was reduced to 57% for Formula F and 36% for Formula G. All these observations suggest that the dissolution- and permeability-enhancing mechanisms of SC, as elaborated earlier, are capable of providing more uniform absorption of OA in the gastrointestinal tract, as reflected by the lower RSD values for the relative bioavailability data. While the particular benefits of SC to the intestinal absorption of OA could not be unequivocally demonstrated in the present study due to its relatively transient action, it should be noted that both Formulas F and G did indeed display a significantly better bioavailability than the commercial tablet, as judged by their lower T_{max}, higher C_{max}, and higher $AUC_{0\rightarrow t}$ (Table 7).

4. Conclusions

Amorphization of OA, a BCS Class IV compound, with polymeric PVP-40 as stabilizer and SC as wetting agent and penetration enhancer by SFD processing yielded kinetically stable solid dispersions with superior dissolution performance, and better and more uniform absorption in comparison with commercial OA tablet. Relative to the SC-free SFD-processed formulation, the SC-containing OA dispersion system showed a higher absorption rate but essentially the same extent of OA absorption. The commercial OA tablet and SFD-processed OA formulations generally displayed large absorption variability, consistent with the absorption characteristics of BCS Class IV compounds. The observed absorption variability of OA could be substantially lessened by inclusion of SC and the use of the sodium salt, OA-Na, in the formulation. Above results suggested that improvement in both aqueous dissolution rate and intestinal permeability of BCS Class IV drugs, as exemplified by the SFD-processed OA-Na/PVP/SC system, is critical to reducing the considerable inter-individual variability in oral absorption commonly observed with this class of compounds.

Acknowledgement

Financial support from the Macao Science and Technology Development Fund (FDCT Fund Project No: 005/2007/A1) is gratefully acknowledged.

References

Amidon, G.L., Lennernas, H., Shah, V.P., Crison, J.R., 1995. A theoretical basis for a biopharmaceutics drug classification: the correlation of *in vitro* drug product dissolution and *in vivo* bioavailability. Pharm. Res. 12, 413–420.

Badens, E., Majerik, V., Horvath, G., Szokonya, L., Bosc, N., Teillaud, E., Charbit, G., 2009. Comparison of solid dispersions produced by supercritical antisolvent and spray-freezing technologies. Int. J. Pharm. 377, 25–34.

Chen, Y., Liu, J., Yang, X., Zhao, X., Xu, H., 2005. Oleanolic acid nanosuspensions: preparation, *in-vitro* characterization and enhanced hepatoprotective effect. J. Pharm. Pharmacol. 57, 259–264.

Chow, K., Tong, H.H.Y., Lum, S., Chow, A.H.L., 2008. Engineering of pharmaceutical materials: an industrial perspective. J. Pharm. Sci. 97, 2855–2877.

Hu, J., Rogers, T.L., Brown, J., Young, T., Johnston, K.P., Williams III, R.O., 2002. Improvement of dissolution rates of poorly water soluble APIs using novel spray freezing into liquid technology. Pharm. Res. 19, 1278–1284.

Hu, J., Johnston, K.P., Williams III, R.O., 2003. Spray freezing into liquid (SFL) particle engineering technology to enhance dissolution of poorly water soluble drugs:

organic solvent versus organic/aqueous co-solvent systems. Eur. J. Pharm. Sci. 20, 295–303.
Hu, J., Johnston, K.P., Williams III, R.O., 2004a. Rapid dissolving high potency danazol powders produced by spray freezing into liquid process. Int. J. Pharm. 271, 145–154.
Hu, J., Johnston, K.P., Williams III, R.O., 2004b. Stable amorphous danazol nanostructured powders with rapid dissolution rates produced by spray freezing into liquid. Drug Dev. Ind. Pharm. 30, 695–704.
Jeong, D.W., Kim, Y.H., Kim, H.H., Ji, H.Y., Yoo, S.D., Choi, W.R., Lee, S.M., Han, C.K., Lee, H.S., 2007. Dose-linear pharmacokinetics of oleanolic acid after intravenous and oral administration in rats. Biopharm. Drug Dispos. 28, 51–57.
Karalis, V., Macheras, P., Peer, A.V., Shah, V.P., 2008. Bioavailability and bioequivalence: focus on physiological factors and variability. Pharm. Res. 25, 1956–1962.
Maa, Y.F., Nguyen, P.A., 2001. Methods of spray freeze drying proteins for pharmaceutical administration. United States Patent 6,284,282.
Maher, S., Leonard, T.W., Jacobsen, J., Brayden, D.J., 2009. Safety and efficacy of sodium caprate in promoting oral drug absorption: from *in vitro* to the clinic. Adv. Drug Deliv. Rev. 61, 1427–1449.
Millqvist-Fureby, A., Malmsten, M., Bergenstahl, B., 1999. Spray drying of trypsin V: surface characterisation and activity preservation. Int. J. Pharm. 188, 243–253.
Najar, I.A., Sachin, B.S., Sharma, S.C., Satti, N.K., Suri, K.A., Johri, R.K., 2010. Modulation of P-glycoprotein ATPase activity by some phytoconstituents. Phytother. Res. 24, 454–458.
Namani, T., Walde, P., 2005. From decanoate micelles to decanoic acid/dodecylbenzenesulfonate vesicles. Langmuir 21, 6210–6219.
Neu, V.T., Zhao, H.R., 2003. Preparation of oleanolic acid solid dispersion systems and their dissolution *in vitro*. J. Chin. Pharm. Univ. 34, 236–239.
Raoof, A.A., Ramtoola, Z., McKenna, B., Yu, R.Z., Hardee, G., Geary, R.S., 2002. Effect of sodium caprate on the intestinal absorption of two modified antisense oligonucleotides in pigs. Eur. J. Pharm. Sci. 17, 131–138.
Rogers, T.L., Hu, J., Yu, Z., Johnston, K.P., Williams III, R.O., 2002a. A novel particle engineering technology: spray-freezing into liquid. Int. J. Pharm. 242, 93–100.
Rogers, T.L., Nelsen, A.C., Hu, J., Brown, J.N., Sarkari, M., Young, T.J., Johnston, K.P., Williams III, R.O., 2002b. A novel particle engineering technology to enhance dissolution of poorly water soluble drugs: spray-freezing into liquid. Eur. J. Pharm. Biopharm. 54, 271–280.
Rogers, T.L., Johnston, K.P., Williams III, R.O., 2003a. Physical stability of micronized powders produced by spray-freezing into liquid (SFL) to enhance the dissolution of an insoluble drug. Pharm. Dev. Technol. 8, 187–197.
Rogers, T.L., Overhoff, K.A., Shah, P., Santiago, P., Yacaman, M.J., Johnston, K.P., Williams III, R.O., 2003b. Micronized powders of a poorly water soluble drug produced by a spray-freezing into liquid-emulsion process. Eur. J. Pharm. Biopharm. 55, 161–172.
Serajuddin, A.T., Thakur, A.B., Ghoshal, R.N., Fakes, M.G., Ranadive, S.A., Morris, K.R., Varia, S.A., 1999. Selection of solid dosage form composition through drug-excipient compatibility testing. J. Pharm. Sci. 88, 696–704.
Sharma, P., Varma, M.V.S., Chawla, H.P.S., Panchagnula, R., 2005. *In situ* and *in vivo* efficacy of peroral absorption enhancers in rats and correlataion to in vitro mechanistic studies. II. Farmaco 60, 874–883.
Sugibayashi, K., Onuki, Y., Takayama, K., 2009. Displacement of tight junction proteins from detergent-resistant membrane domains by treatment with sodium caprate. Eur. J. Pharm. Sci. 36, 246–253.
Tong, H.H.Y., Wu, H.B., Zheng, Y., Xi, J., Chow, A.H.L., Chan, C.K., 2008. Physical characterization of oleanolic acid nonsolvate and solvates prepared by solvent recrystallization. Int. J. Pharm. 355, 195–202.
United States Food and Drug Administration, 2009. Code of Federal Regulations Title 21 Food and Drugs Chapter I Food and Drug Administration Department of Health and Human Services Subchapter B Food for Human Consumption (continued) Part 172 Food Additives Permitted for Direct Addition to Food for Human Consumption. Food and Drug Administration, Rockville, United States.
United States Food and Drug Administration, 2000. Guidance for Industry: Waiver of in vivo Bioavailability and Bioequivalence Studies for Immediate-Release Solid Oral Dosage Forms Based on a Biopharmaceutics Classification System. Food and Drug Administration, Rockville, United States.
Vaughn, J.M., McConville, J.T., Crisp, M.T., Johnston, K.P., Williams III, R.O., 2006. Supersaturation produces high bioavailability of amorphous danazol particles formed by evaporative precipitation into aqueous solution and spray freezing into liquid technologies. Drug Dev. Ind. Pharm. 32, 559–567.
Williams III, R.O., Johnston, K.P., Young, T.J., Rogers, T.L., Barron, M.K., Yu, Z., Hu, J., 2005. Process for production of nanoparticles and microparticles by spray freezing into liquid. United States Patent 6,862,890.
Xi, J., Chang, Q., Chan, C.K., Meng, Z.Y., Wang, G.N., Sun, J.B., Wang, Y.T., Tong, H.H.Y., Zheng, Y., 2009. Formulation development and bioavailability evaluation of a self-nanoemulsified drug delivery system of oleanolic acid. AAPS PharmSciTech. 10, 172–182.
Yan, Y.D., Feng, B., Huang, X.J., Zhou, Z.G., 1995. Study on β-cyclodextrin inclusion compound of oleanolic acid. Chin. Tradit. Patent Med. 6, 2–4.
Zhang, L., Zheng, Y., Chow, M.S.S., Zuo, Z., 2004. Investigation of intestinal absorption and disposition of green tea catechins by Caco-2 monolayer model. Int. J. Pharm. 287, 1–12.
Zhou, L., Chow, M.S.S., Zuo, Z., 2009. Effect of sodium caprate on the oral absorptions of danshensu and salvianolic acid B. Int. J. Pharm. 379, 109–118.